 doi:10.20944/preprints202004.0020.v1

*Article*

# Experimental and Numerical Evaluation of Residual Displacement and Ductility in Ratcheting and Shakedown of an Aluminium Beam

**Simone Palladino [1], Luca Esposito [2], Paolo Ferla [3], Elena Totaro [4], Renato Zona [5] and Vincenzo Minutolo [6]***

[1] University of Campania "Luigi Vanvitelli"; simone.palladino@unicampania.it
[2] University of Campania "Luigi Vanvitelli"; luca.esposito@unicampania.it
[3] University of Campania "Luigi Vanvitelli"; paolo.ferla@unicampania.it
[4] University of Campania "Luigi Vanvitelli"; elena.totaro@unicampania.it
[5] University of Campania "Luigi Vanvitelli"; renato.zona@unicampania.it
[6] University of Campania "Luigi Vanvitelli"; vincenzo.minutolo@unicampania.it
* Correspondence: vincenzo.minutolo@unicampania.it; Tel.: +39-081-5010-305

**Abstract:** Safety assessment of structures can be obtained by means of limit design in order to overcome uncertainties concerning actual response due to inelastic constitutive behaviour and more generally to non-linear structural response and loads' random variability. The limit analysis is used for evaluating the safety of the structures directly starting from load level without any knowledge of the load history. In the paper, the lower bound calculation is proposed based on permanent strain parametric description of the residual stress. The strategy allows considering the permanent strain as the effective parameters of the procedure and can be used to control the ductility requirements until complete load program develops. In this way one can control if the structure can develop entirely its possibility of plastic adaptation up to required load level. The procedure is compared to experimental results obtained on aluminium beams in shake down.

**Keywords:** shakedown; plasticity; limit design; ratcheting, experimental comparison, residual displacement

## 1. Introduction

Actual application of structural analysis deals with complex constructions subjected to randomly variable loads. Generally, the load intensity bounds are prescribed by standards and authorities and are evaluated starting from probabilistic and statistical considerations. It is almost impossible, in practical cases, to know actual load history and their distribution all over the structure considering that only their intensity range is estimated.

Under these hypotheses, evaluating structural safety is a matter of overall consideration rather than specific pointwise calculation of the response.

Under the above quoted circumstances, the main strategy for structural safety assessment is the calculation of load collapse limit, both under proportionally and randomly variable cases [1, 2].

The first case cited above concerns the usual collapse limit and the latter can be ascribed to shakedown limit definition. In this second situation, some specification should be done on the velocity of the phenomenon in order to distinguish between elastic and plastic shakedown propagation, but here only statics will be considered [3, 4, 5].

Generally, the knowledge of the structural limit load is pursued by means of step by step or limit analyses. This latter method is based on the two forms coming from the upper bound and of the lower

bound theorems. These theorems are based on kinematic and static approach respectively. The first is aimed calculating the limit load as the maximum among any statically admissible loads and the second as the minimum among any kinematically admissible loads. Both calculations are independent from actual load histories, and although this is useful in the real-life analysis where the loads are known only in term of their intensity bounds, it constitutes a limitation for the use of the method since it cannot evaluate the dissipation during ultra-elastic deformation. It is possible, therefore, that the permanent deformation, required for the ultra-elastic load path to develop, attains its limit prior the collapse. Such an eventuality causes the limit analysis fail since the collapse occurs before the complete permanent deformation develops. This happens at an actual load level lower that the theoretical limit.

This disadvantage is only apparently overcoming by the step-by-step analysis since this approach is linked to the knowledge of the actual load history and gives results that cannot be generalized.

In modern application of structural engineering, numerical formulation of the limit analysis allows the application of the methods to a wide class of structure. In particular, the Finite Element Method has wide application to two- and three-dimensional structures. In [6, 7] shakedown analysis for elastic-perfect plastic frames is discussed and an incremental-iterative solution is proposed. A general procedure dealing with finite element application for lower bound determination of collapse and ratcheting load is in [8]. As stated before, one of the most important weakness of limit analysis is that no direct information is given by the theoretical fundamentals of the analysis about the dissipation during the deformation process. It has to be stressed that one of the hypotheses at the basis of the limit design is that the strain can develop completely until the load reaches its limit, namely the permanent strain has to be limited within the admissible amount. Only the knowledge of the load history allows evaluating precisely the amount of dissipated energy until the limit is attained.

Hence, many works estimate the ultimate dissipation and displacements during plastic loading of structures at the incoming plastic collapse or to ratcheting [9, 10, 11] starting from Ponter that proposes a limit on the dissipated work and residual displacement [12, 13]. In the present work, a procedure has been presented through the Melàn's theorem [14] of shake down. The procedure has used the "strain-based residual" stress that constitutes a basis of the vector space of the self-equilibrated stresses. Such a residual stress fulfils the Mèlan's lower bound theorem and has been used to calculate upper bounds of the global and local dissipated work at the ultimate load level and pointwise permanent strain as well.

The method has proposed, in the framework of discontinuous FEM, a linear optimization strategy that gives an upper bound of local dissipation and finally an estimate of local permanent displacement. In the paper, the numerical procedure has been applied to some academic examples of frame structures and to 2D plates structures. With reference to one dimensional example, the numerical procedure was compared also to the experimental results obtained by the authors in a previous work [15]. The experiment has concerned an aluminium beam over three supports, loaded by randomly variable one-point forces applied at the middle of each span. The structure has been loaded up to shake down limit and subsequently to ratcheting. The displacement has been measured during the loading process. The experimental results have been compared with the calculated ones and a good agreement has been shown between theoretical and experimental approaches.

## 2. Fundamentals of limit analysis.

A structure collapses if the dissipation due to permanent deformation increases in time indefinitely. The dissipation increment can be produced by proportional increasing loads hence proper proportional collapse occurs. With no difference, the dissipation can increase in time alternating periods when no dissipation occurs and periods when dissipation get further increase. In this latter case it is possible that either the displacement become excessive for functionality and safety

Preprints (www.preprints.org) | NOT PEER-REVIEWED | Posted: 3 April 2020 doi:10.20944/preprints202004.0020.v1



or the total dissipation reaches a limit that produces the material failure. The first is the ratcheting phenomenon the second the plastic fatigue rupture (also known as low cycle number fatigue) [16].

In order to evaluate the load collapse limit, the static collapse theorem states that: if under actual loads there exists any equilibrated stress that definitely belongs to the elastic domain, the permanent strain rate vanishes with time increasing, hence collapse does not occur [1]. In better word the structure does stabilize, i.e. the structure behaves as to be elastic after a certain amount of permanent strain has been accumulated. Moreover a limiting equation exists that gives an upper bound of the dissipated energy till stabilization if any [13, 17].

The present work has described a numerical procedure that implemented the Melan theorem. For the sake of completeness, the Melan theorem has been reported here after briefly.

Let us consider a structure that occupies a domain $\Omega$ with the boundary $\partial\Omega$. The structure is in equilibrium under prescribed body forces, $b_i$, in the interior of the solid, $\overset{o}{\Omega}$, and prescribed tractions, $t_i$, on the part of the boundary $\partial\Omega_f$; both forces vary in time within prescribed limit with absolutely random time law. On the part of the boundary $\partial\Omega_u = \partial\Omega \backslash \partial\Omega_f$ the displacement is prescribed [18]. Due to the applied loads and displacements, the solid present the stress, $\sigma_{ij}$ and the strain, $\varepsilon_{hk}$, in the interior and reactive tractions, $t_i^s$, on the boundary $\partial\Omega_u$. In the following, indicial notation is adopted hence a subscript $_i$ have denoted the $i^{th}$ component of a vector with respect to the reference frame, two subscripts have referred to the two components of a second order tensor and so on; moreover, subscripts following the comma indicate partial derivatives with respect to the coordinate directions.

A self-equilibrated stress, $\rho_{ij}$, is a stress field that satisfies the homogeneous balance equations and the corresponding homogeneous natural boundary conditions on the loaded boundary $\partial\Omega_f$. Only on the constrained boundary $\partial\Omega_u$ tractions can be non-null:

$$\begin{aligned} &\rho_{ij,j} = 0 \; in \; \Omega \\ &\rho_{ij} n_j = 0 \; on \; \partial\Omega_f \\ &\rho_{ij} n_j = t_i^s \; on \; \partial\Omega_u \end{aligned} \tag{1}$$

The material constituting the structure is elastic-perfectly plastic, so the stress-strain law is:

$$\sigma_{ij} = S_{ijhk}(\varepsilon_{hk} - p_{hk}) \tag{2}$$

where $S_{ijhk}$ is the elastic forth order tensor.

The permanent strain, $p_{hk}$, results from the integration during the load process of the permanent strain rate, $\dot{p}_{hk}$, that is related to the stress by means of the constitutive associated flow rule:

$$\begin{cases} f(\sigma_{ij}) = 0 \\ \dfrac{\partial f}{\partial \sigma_{ij}} \dot{\sigma}_{ij} = 0 \end{cases} \Leftrightarrow \dot{p_{hk}} = \dot{\lambda} \frac{\partial f}{\partial \sigma_{ij}} \tag{3}$$

where $f(\sigma_{ij}) \leq 0$ is the compatibility condition on stress, equality holds for yielding.

The actual strain field can be represented accordingly to the following additive decomposition:

$$\varepsilon_{hk} = {\varepsilon_{hk}}^E + {\varepsilon_{hk}}^P + p_{hk} \tag{4}$$

where, under the small displacements hypothesis actual strain, $\varepsilon_{hk}$, is obtained by the superimposition of the elastic, ${\varepsilon_{hk}}^E$, the elastic-plastic, ${\varepsilon_{hk}}^P$ and the permanent strain, $p_{hk}$.

The equilibrated stress, in term of the self-equilibrated residual stresses $\rho_{ij}$ and the pure elastic stress is obtained by the following additive decomposition as well:

$$\sigma_{ij} = \sigma_{ij}^E + \rho_{ij} \tag{5}$$

Namely, the stress tensor, $\sigma_{ij}$, is decomposed into two parts, the elastic part, $\sigma_{ij}^E$, and the elastic-plastic part, $\rho_{ij}$ analogously to the strain in (4). The only difference is that no discontinuous part of the stress is present playing the role of $p_{hk}$:

Preprints (www.preprints.org) | NOT PEER-REVIEWED | Posted: 3 April 2020 doi:10.20944/preprints202004.0020.v1



$$\sigma_{ij}^{E} = S_{ijhk}{\varepsilon_{hk}}^{E}$$
$$\rho_{ij} = S_{ijhk}{\varepsilon_{hk}}^{P} \quad (6)$$

The strain $\varepsilon_{hk}^{P}$ represents the elastic strain that, in conjunction with permanent strain, $p_{hk}$, forms a kinematically compatible strain field in $\Omega$. It is useful to remind that separately $p_{hk}$ and $\varepsilon_{hk}^{P}$ do not satisfy kinematical compatibility but their sum does constitute a compatible strain.

Because of its definition, the stress $\sigma_{ij}^{P}$ is a self-equilibrated stress. Indeed, the equilibrium equation of the interior points of the solid body involves the divergence operator of the stress:

$$\sigma_{ij,j} + b_i = 0 \quad (7)$$

By using equation (6), the equilibrium of internal points become:

$$\left(S_{ijhk}\,\varepsilon_{hk,j}^{E} + S_{ijhk}{\varepsilon_{hk,j}}^{P}\right) + b_i = 0 \quad (8)$$

The elastic stress is the stress in equilibrium in $\Omega$, when constitutive equation is assumed to be indefinitely elastic, subjected to the same loads than the actual structure. Consequently, the pure elastic stress is in equilibrium with the applied forces so that the following equation holds true:

$$(S_{ijhk,j}\,\varepsilon_{hk,j}^{E}) + b_i = 0 \quad (9)$$

Comparing equation (8) with (9) the following equation is obtained confirming that the elastic-plastic stress is self-equilibrated in the interior of the structure.

$$S_{ijhk}{\varepsilon_{hk,j}}^{P} = 0 \quad (10)$$

Moreover, the self-equilibrated stress satisfies the homogeneous boundary condition on free boundary of the structure. Finally, the equilibrium equation involving the stress $\rho_{ij,j}$ reduce to equation (1).

The above reasoning can be summarized as follows: the actual elastic-plastic stress solution, resulting from applied body and boundary loads, differs from the pure elastic stress by a self-equilibrated stress. This self-equilibrated stress is due to permanent elastic strain $\dot{\varepsilon}_{hk}^{P}$ that results from compatibility equation with respect to the permanent discontinuous strain $p_{hk}$ acting as Volterra's dislocation. Dislocations are the kinematical effect resulting in discontinuities of strain within the structure. A dislocation causes that stress arise in the absence of loads. The stress produced by dislocation is hence an eigenstress and satisfy equations (1) and equation (11). The stress $\rho_{ij}$, that depends on $\dot{\varepsilon}_{hk}^{P}$, through equation (10), emerges on the constrained boundary as the self-equilibrated traction, $t_i^s$.

$$\rho_{ij} n_j = t_i^s \; on \; \partial\Omega_u \quad (11)$$

## 3. Lower bound limit analysis

The shakedown is the phenomenon where under randomly repeated loads, the structure undergoes to elastic behaviour definitely for increasing time. In other word the permanent strain rate $\dot{p}_{hk}$ approaches zero for t→∞ hence the permanent strain is bounded in time.

The existence of shakedown is ruled by the Mèlan's theorem. The theorem is formulated in term of self-equilibrated stress of the form $\rho_{ij}$.

The line of reasoning of the Melan's theorem is suitable as well for the application to the proportional collapse analysis.

In the following formulation the $\rho_{ij}$ is obtained from the $p_{hk}$ as the resulting stress from the application of the $p_{hk}$ as a Volterra's dislocation.

The operator $Z_{ijhk}$ governs the relationship between $p_{hk}$ and $\rho_{ij}$:

$$\rho_{ij} = Z_{ijhk}\, p_{hk} \quad (12)$$

Preprints (www.preprints.org) | NOT PEER-REVIEWED | Posted: 3 April 2020 doi:10.20944/preprints202004.0020.v1



The condition of shakedown is stated by the Mèlan's theorem in the following form: stabilization occurs under a load multiplier $k$ if and only if there exists a self-equilibrated stress $\rho_{ij}$, time independent called eigenstress, such that:

$$f\left(k\, C_{ijhk}\varepsilon^{E}_{hk} + \rho_{ij}\right) \leq 0 \tag{13}$$

at any time.

By considering equation (12) the Mèlan's theorem is satisfied if there exists a permanent strain ${p_{hk}}^{r}$ such that

$$f\left(k\, C_{ijhk}\varepsilon^{E}_{hk} + Z_{ijhk}\, {p_{hk}}^{r}\right) < 0\ . \tag{14}$$

The search of the limit, either collapse or shakedown, load can be stated by considering the maximum "s" of k under the constraints (14).

The optimization program that searches for the load limit multiplier is summarised in:

$$\text{find} \sup_{P^{r}_{hk}} k \,\Big|\, f\left(k\, C_{ijhk}\varepsilon^{E}_{hk} + Z_{ijhk}\, {p_{hk}}^{r}\right) < 0 \tag{15}$$

The program (15) is linear provided the constraint, constituted by compatibility inequality, is linear. In the other cases it constitutes a non-linear programming statement.

The solution of the program (15) is the limit collapse multiplier that is either the proportional collapse multiplier, $s_c$, or the shakedown limit, $s_s$, provided the elastic stress corresponds to monotone or variable loads, moreover the program furnishes a set of permanent time independent strain ${p_{hk}}^{r}$ satisfying the theorem.

The ${p_{hk}}^{r}$ are the Mèlan's residuals, and do not constitutes the actual residual strain that depends on the undefined load path.

As a corollary of the Mèlan's theorem, see Koiter and Koning [1, 19, 16], an upper bound on total dissipated energy until stabilization is obtained as a function of the elastic strain energy corresponding to the Mèlan's residual strain, ${p_{ij}}^{r}$.

$$\int_0^{\infty}\int_{\Omega}\sigma_{ij}\dot{p}_{ij}\, dVdt \leq \frac{m}{2(m-1)}\int_{\Omega} S_{hkij}\,\rho^{r}_{ij}\,\rho^{r}_{hk}\, dV \tag{16}$$

where the term on the left-hand side of equation (16) is the total dissipation at the incoming collapse.

$$D = \int_0^{\infty}\int_{\Omega}\sigma_{ij}\dot{p}_{ij}\, dVdt \tag{17}$$

the right-hand side contains the strain energy of the Melan's residual stress

$$W = \frac{1}{2}\int_{\Omega} S_{hkij}\,\rho^{r}_{ij}\,\rho^{r}_{hk}\, dV \tag{18}$$

and the safety coefficient of the actual load multiplier with respect to the considered collapse:

$$m = \frac{k}{s_l}, s_l = \begin{cases} s_c \\ s_s \end{cases} \tag{19}$$

The equation (17) constitutes, for any load factor, $m$, a constraint the permanent strain $\dot{p}_{ij}$ must satisfy. It is, then, possible to define a second optimization program by remembering equation (12):

$$\text{find} \sup_{P^{r}_{hk}} p_{rs}(\boldsymbol{x}) \,\Bigg|\, \begin{matrix} f\left(m\, s_l\, C_{ijhk}\varepsilon^{E}_{hk} + Z_{ijhk}\, p^{r}_{hk}\right) < 0 \\ \int_{\Omega}\sigma_{ij}p_{ij}\, dV \leq \frac{m}{2(m-1)}\int_{\Omega} Z_{hkij}\, p^{r}_{hk}p^{r}_{ij}\, dV \end{matrix} \tag{20}$$

that can be used to calculate residual displacement upper-bound at a specific point, $\boldsymbol{x}$, of the structure. In equation (20) the objective function can be any linear combination of the permanent strain; hence any displacement can be calculated by means of (20) even if it is not a variable of the inequalities provided linear relationship holds between displacements and dislocations.

Preprints (www.preprints.org) | NOT PEER-REVIEWED | Posted: 3 April 2020 doi:10.20944/preprints202004.0020.v1



**4. Results**

The described method has been applied to structures made of one-dimensional beams. The beams are plane and are subjected to flexural loads. Shear effects are negligible so that only bending moment has been considered. The compatibility condition has reduced to simple limitation of the bending moment, namely

$$M_y^- < M < M_y^+ \tag{21}$$

In equation (21), $M_y^{-/+}$ represents the negative and the positive limit bending moment of the beam cross section respectively.

In order to compare the results with the experimental ones presented in [15], the experiment is briefly recalled. The tested structure was an aluminium beam, over three supports. The supports were equally spaced, the beam was loaded by one-point forces applied at the middle of each span. The forces $F_1$, $F_2$, has varied accordingly with the load program whose diagram has been drawn in Figure 1.

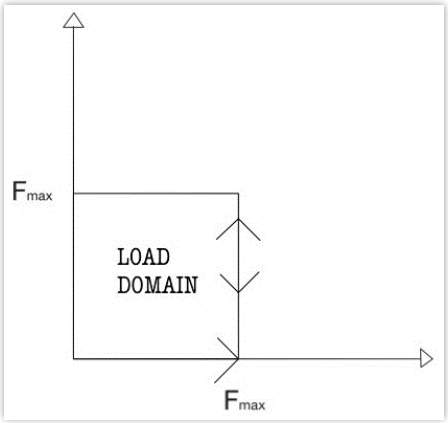


**Figure 1** Loading Domain

The structural scheme of the specimen is depicted in Figure 2 where the half span length was:

$$l = 400mm$$

The mechanical constitutive constants of the specimen were reported in 错误!未找到引用源。 where only the average of the parameters. The upper bound of the load programs, $F_{max}$, has been progressively increased from the elastic limit to ratcheting. During the test the displacement was recorded at any load step. It has been possible, consequently, to see that for loads within the shakedown limit, the displacement did stabilize after a few load cycles. Conversely when the load bound was comprised between the shakedown and the collapse limits, the displacement average has increased in time. Finally, when the load equated or overcame the collapse limit, the structure did fail.

The experimental report has furnished the relevant parameters of the material constituting the beam and the limit bending moment has been calculated considering the experimental results. It has to be considered that some buckling of the cross section of the beam occurs, the effects have been neglected in present work, although they could be considered [20, 21].

**Table 1**: Material parameters

| Mechanical constant | Range of values |
|---|---|

Preprints (www.preprints.org) | NOT PEER-REVIEWED | Posted: 3 April 2020 doi:10.20944/preprints202004.0020.v1



| | |
|---|---|
| Young modulus E | $6250 - 6400\ Mpa$ |
| Limit bending moment $M_0$ | $0.3276 - 0.3324 kNm$ |
| Yield stress $\sigma_Y$ | $193.16 - 196.00\ Mpa$ |

The same structure has been analysed by means of the Melan's theorem accordingly to the proposed procedure. The results, reported in the following, allowed to recognize that theoretical load limits were in good agreement with the experimental results. Moreover, the dissipation limitation, equation (16), has been used to calculate the upper bound limit of the displacement of the point D where the force was applied. The resulting calculated upper bound of the displacement has been compared with the measured one during the experiment. It has been shown that theoretical forecast and actual results were in good agreement as it can be seen in **Table 4**.

*4.1 Numerical results*

The considered aluminium beam had following scheme:

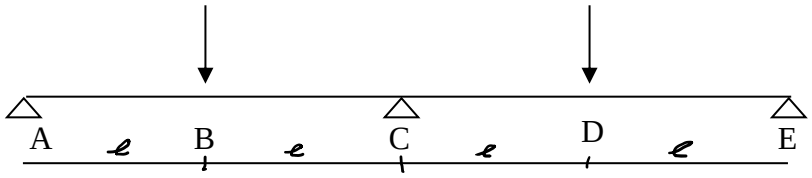


Figure 2: Structural scheme, loading position and constraints.

The cross-section of the beam was box shaped as reported in [15] where the meaningful parameters have been highlighted.

For the calculation of structures under bending, the formulation reported in the previous sections has been rewritten with reference to generalized stress and strain.

The generalized strain should be intended as the slope of the beam's axis moreover the stress has to be represented by the bending moment, $M$. Finally, the permanent discontinuous strain, $p_{hk}$, must be considered as the localized rotation discontinuity, $\Delta\varphi$.

Whit the above introduced quantities the optimization program, equation (15), modifies in the following way:

$$\underset{\Delta\varphi}{\text{Sup}}\ \text{k} \begin{vmatrix} -Z\Delta\varphi - kM^{min} < |M_y^-| \\ Z\Delta\varphi + kM^{max} < |M_y^+| \end{vmatrix} \tag{22}$$

In equation (22), $M^{max}$ is the maximum bending moment and $M^{min}$ is the minimum bending moment produced by the applied loads during the load path. The moments in several points, say A, B, C and D, are collected in a single vector, so are the residual rotations $\Delta\varphi$, so that the equation (22) results in a matrix form linear inequality system. The choice of the control points (A, B, C and D) was dependent on the prediction of the local extrema of the internal stress. It must be stressed that whether the stress should violate the compatibility equation at points not comprised in the control set the results will overestimate the load multiplier. Consequently, one must consider setting up the procedure that will converge from below in the domain of self-equilibrated stress but will converge from above with the increase of the control points. In the proposed example, however, the position of the control points ensured that the compatibility was fulfilled everywhere in the structure.

The mechanical parameters and the geometry of the beam have been introduced into the calculation of the operator $\boldsymbol{Z}$. Since the formulation in term of generalized vectors of rotations and bending moments, the operator assumes the form of a square matrix here called influence matrix. The influence matrix can be calculated directly in case of one-dimensional structures applying the definition given in equation (12). The particularization of Equation (12) to the case of beams in bending has given the following equation:

Preprints (www.preprints.org) | NOT PEER-REVIEWED | Posted: 3 April 2020 doi:10.20944/preprints202004.0020.v1



$$M^r = Z\Delta\varphi \tag{23}$$

where the $\boldsymbol{Z}$ matrix contains the bending moment at the end point of any beams due to a slope discontinuity applied to any other beam end points.

In the proposed example the beams and the corresponding points have been numbered as represented in Figure 3. Henceforth the element $Z_{ij}$ of $\boldsymbol{Z}$ has the meaning of the bending moment at $P_i$ due to the rotation $\Delta\varphi_j$ at $P_j$.

To calculate an upper bound of the residual displacements on the structure at shakedown, the program Equation (20) has been rewritten accordingly to the position (22) becoming:

$$\text{find} \sup_{\Delta\varphi} \Delta\varphi_i^{+/-} \left| \begin{array}{c} -Z\Delta\varphi - \frac{s_{sd}}{m} M^{min} < \left|M_y^-\right| \\ Z\Delta\varphi + \frac{s_{sd}}{m} M^{max} < \left|M_y^+\right| \\ M_y^- \cdot \Delta\varphi^- + M_y^+ \cdot \Delta\varphi^+ \leq \frac{m}{2(m-1)} \Delta\varphi^T Z \Delta\varphi \end{array} \right. \tag{24}$$

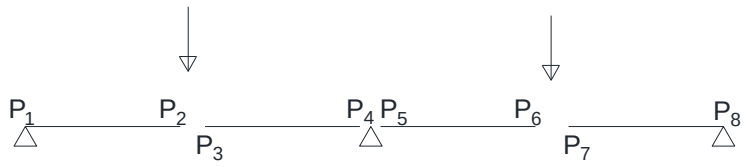


**Figure 3**: Sample point numbering and position

The resulting Z, obtained through the assigned data was:

$$Z = \begin{vmatrix} 0 & 0 & 0 & 0 & 0 & 0 & 0 & 0 \\ 0 & -4{,}18E{+}05 & -4{,}18E{+}05 & -8{,}36E{+}05 & -8{,}36E{+}05 & -4{,}18E{+}05 & -4{,}18E{+}05 & 0 \\ 0 & -4{,}18E{+}05 & -4{,}18E{+}05 & -8{,}36E{+}05 & -8{,}36E{+}05 & -4{,}18E{+}05 & -4{,}18E{+}05 & 0 \\ 0 & -8{,}36E{+}05 & -8{,}36E{+}05 & -1{,}67E{+}06 & -1{,}67E{+}06 & -8{,}36E{+}05 & -8{,}36E{+}05 & 0 \\ 0 & -8{,}36E{+}05 & -8{,}36E{+}05 & -1{,}67E{+}06 & -1{,}67E{+}06 & -8{,}36E{+}05 & -8{,}36E{+}05 & 0 \\ 0 & -4{,}18E{+}05 & -4{,}18E{+}05 & -8{,}36E{+}05 & -8{,}36E{+}05 & -4{,}18E{+}05 & -4{,}18E{+}05 & 0 \\ 0 & -4{,}18E{+}05 & -4{,}18E{+}05 & -8{,}36E{+}05 & -8{,}36E{+}05 & -4{,}18E{+}05 & -4{,}18E{+}05 & 0 \\ 0 & 0 & 0 & 0 & 0 & 0 & 0 & 0 \end{vmatrix}$$

**Table 2** Step by step results by present model

| F[kN] | Vres [0.4 m] | Δϕp | D [kN*m] |
|---|---|---|---|
| 2.03 | $6.52 * 10^{-4}$ | $5.21 * 10^{-3}$ | $1.70 * 10^{-3}$ |
| 2.06 | $2.074 * 10^{-3}$ | 0.0166 | $5.44 * 10^{-3}$ |
| 2.065 | $2.34 * 10^{-3}$ | 0.0187 | $6.14 * 10^{-3}$ |
| 2.07 | $2.578 * 10^{-3}$ | 0.0206 | $6.76 * 10^{-3}$ |
| 2.08 | $3.052 * 10^{-3}$ | 0.0244 | $8.00 * 10^{-3}$ |
| 2.09 | $3.52 * 10^{-3}$ | 0.0282 | $9.24 * 10^{-3}$ |

In order to verify the results of the previous approach, collapse multipliers have been calculated through the Koiter's kinematical approach and chosen as the min values of them and equal to $\gamma$=10.1.

In fact, the yield force has been calculated as the force corresponding to the minimum multiplier between the loading scheme $F_1$, $F_2$ and $F_1$+$F_2$ as reported in the following steps:

Preprints (www.preprints.org) | NOT PEER-REVIEWED | Posted: 3 April 2020 doi:10.20944/preprints202004.0020.v1



Under the application of a single $F_1$=$F_2$ force in the middle of the left/right span, the multiplier's value resulted:

$$\gamma = 10.1\frac{M_y}{FL} \tag{25}$$

The multipliers $\gamma_1$, $\gamma_2$ shown in (25), resulted as the researched minimum kinematic multipliers and shown as follow:

$$\gamma = \frac{10.1My}{L}$$
$$\gamma \in [2.069,2.098]$$

Where $M_y$ has the values reported in Table 1

*3.2 Experimental results*

The experimental analysis reports the displacement record during the load path. In Table 3 the maximum applied load and corresponding displacement of the middle point of the left span of the structure is recorded. The load path consists of a fixed force at nominal value applied to right span and a variable load varying from 0 to the maximum value at the left span as it is depicted in Figure 1

**Table 3:** Experimental Residual displacements from **[15]**

| F[kN] | wres$^B$[mm] t=0 | wres$^2$[mm] t=∞ |
|---|---|---|
| 2.032 | 4.07 | 3.61 |
| 2.069 | 4.67 | 4.32 |
| 2.099 | 5.48 | *5.25* |
| 2.139 | 7.06 | 6.72 |
| 2.180 | 11.42 | 11.31 |

During the experiment, the structure underwent to ratcheting for loads greater than 2.069 kN. The recorded displacement rate did not vanish, and the measured values refers to the end of the experiment. For loading less or equal to 2.069 the displacement rate vanishes since shake down occurs.

The proposed method has been applied to the structure, in particular the program Equation (22) has been used to calculate the shakedown multiplier and the residual rotations.

Moreover the resulting residuals have been introduced to formulate the program equation (24) where the displacement at the middle of the right span has been calculated in term pf the residual rotation giving the result reported in **Table 4**. In the table, the results from actual calculation have been compared with the experiments. The correspondence between the calculation and the measures are rather confirming the effectiveness of the proposed procedure. Moreover, it's possible to notice the comparison between the experimental results and the present one reported in the table 7, where all the loads and the residual displacements that resulted to be in good agreement among them have been reported. In fact, the residual displacements calculated through a numerical procedure, resulted to be an upper bound of the experimental one.

**Table 4:** Comparison between experimental and calculated residual displacements 1 Experimental displacements [15], 2 Calculated displacement assuming My =0.3276 kN m, 3 Calculated displacements assuming My =0.3324 kN m).

Preprints (www.preprints.org) | NOT PEER-REVIEWED | Posted: 3 April 2020 doi:10.20944/preprints202004.0020.v1



| F[kN] | Vres¹[mm] | Vres²[mm] | Vres³[mm] |
|---|---|---|---|
| 2.032 | 3.61 | 4.09 | / |
| 2.069 | 4.32 | / | 6.23 |
| 2.099 | 5.25 | / | / |
| 2.139 | 6.72 | / | / |
| 2.180 | 11.31 | / | / |

Finally, a general diagram about results that have been summarised in the previous Table 4, has been reported in the Figure 4 below:

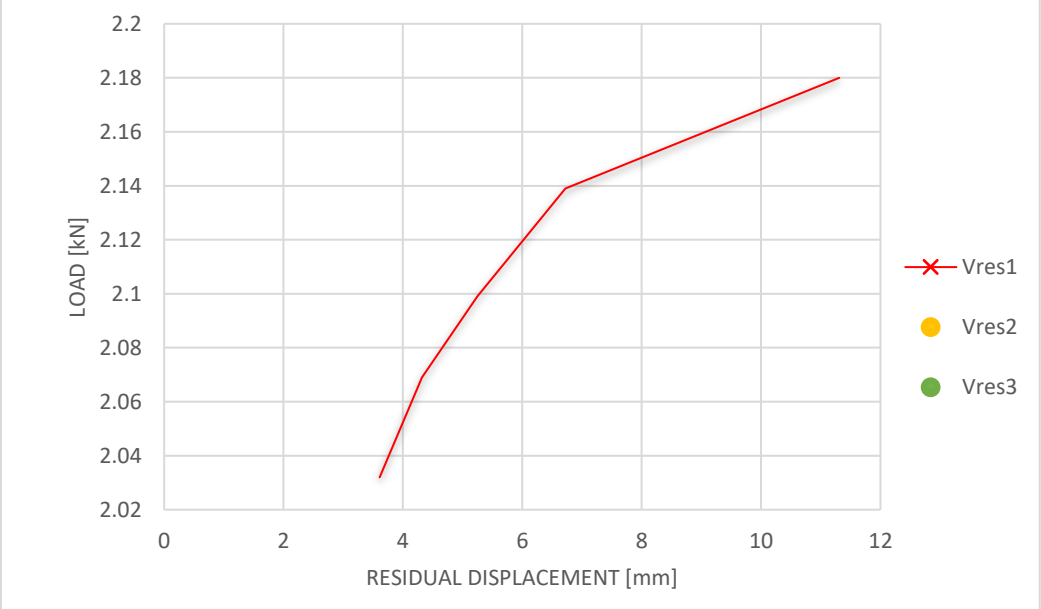


**Figure 4** Comparison between experimental and calculated residual displacements (Red line: Experimental displacements [15], Yellow point: Calculated displacements assuming My=0.3276 kN m, Green point: Calculated displacements assuming My =0.3324 kN m).

## 4. Discussion

The diagram in Figure 4 contain the experimental data derived from that reported in [15]and the calculated data derived from the numerical procedure previously introduced inside the paper. It shows the trend of the displacement with respect to the applied load during the experiment and the comparison with respect to the numerical procedure. In particular it is evident that the displacement increases with the load and showed in the Figure 4 through the orange curve and representing the experimental response. The experimental data have been recorded for loads greater than the shake down limit during ratcheting, the measures have been interrupted after several load cycles. Consequently, the displacement corresponding to load greater than 2.069kN should not be considered. The records corresponding to load lower than 2.069kN has been compared to the upper bound of the displacement obtained by the proposed method with the yellow and green points reported in the Figure 4.

In the Figure 4, it is shown that the experimental residual displacements are limited from above by the calculated results in accordance with the theory of shake down. The proposed method is rather accurate for estimating the residuals in shake down. The procedure can be generalised, as mentioned below to 2D and 3D structures through the definition of the finite element derivation of the Z matrix.

 doi:10.20944/preprints202004.0020.v1



## 5. Conclusions

The calculation carried on using the proposed method furnished an upper bound of the displacement of the mid span of the beam. The obtained results depended on the load level by means of the safety factor *m*. The obtained results compared with the experimental ones from [15]allows confirming the good accuracy of the method and suggest the possibility it is extended to more complex structural engineering. The calculation of the displacement upper-bound is of great importance when structural analysis is applied to seismic engineering. The modern strategy of static nonlinear analysis, achieved through Push-Over procedure [22][OBJ], ], . It is evident that the procedure furnishes a good estimation of the displacement and can be assumed as the basis for the evaluation of ductility performance of the beam. The proposed strategy has been applied limiting to flexural behaviour of beams however it is quite general and can be extended to 2D and 3D structures using FEM formulation.

**Author Contributions:**

Conceptualization, Vincenzo Minutolo, Simone Palladino, Luca Esposito, Paolo Ferla, Elena Totaro and Renato Zona; Data curation, Vincenzo Minutolo, Simone Palladino, Luca Esposito, Paolo Ferla, Elena Totaro and Renato Zona; Formal analysis, Vincenzo Minutolo, Simone Palladino, Luca Esposito, Paolo Ferla, Elena Totaro and Renato Zona; Funding acquisition, Vincenzo Minutolo, Simone Palladino, Luca Esposito, Paolo Ferla, Elena Totaro and Renato Zona; Investigation, Vincenzo Minutolo, Simone Palladino, Luca Esposito, Paolo Ferla, Elena Totaro and Renato Zona; Methodology, Vincenzo Minutolo, Simone Palladino, Luca Esposito, Paolo Ferla, Elena Totaro and Renato Zona; Project administration, Vincenzo Minutolo; Resources, Vincenzo Minutolo, Simone Palladino, Luca Esposito, Paolo Ferla, Elena Totaro and Renato Zona; Software, Vincenzo Minutolo, Simone Palladino, Luca Esposito, Paolo Ferla, Elena Totaro and Renato Zona; Supervision, Vincenzo Minutolo; Validation, Vincenzo Minutolo, Simone Palladino, Luca Esposito, Paolo Ferla, Elena Totaro and Renato Zona; Visualization, Vincenzo Minutolo, Simone Palladino, Luca Esposito, Paolo Ferla, Elena Totaro and Renato Zona; Writing – original draft, Vincenzo Minutolo, Simone Palladino, Luca Esposito, Paolo Ferla, Elena Totaro and Renato Zona; Writing – review & editing, Vincenzo Minutolo, Simone Palladino, Luca Esposito, Paolo Ferla, Elena Totaro and Renato Zona..

**Acknowledgments:** The authors acknowledge the financial grant program VALERE: "VAnviteLli pEr la RicErca"

**Conflicts of Interest:** The authors declare no conflict of interest.

## References

[1] W. T. Koiter, "General theorems for elastic-plastic solids," *Progress in Solid Mechanics,* vol. 1, pp. 165-221, 1960.

[2] J. Lubliner, Plasticity theory, Courier Corporation, 2008.

[3] T. Hassan and S. Kyriakides, "Ratcheting of cyclically hardening and softening materials: I. Uniaxial behavior," *International Journal of Plasticity,* vol. 10, no. 2, pp. 149-184, 1994.

[4] T. Hassan and S. Kyriakides, "Ratcheting of cyclically hardening and softening materials: II. Multiaxial behavior," *International Journal of Plasticity,* vol. 10, no. 2, pp. 185-212, 1994.

[5] N. Mandal, "On the low cycle fatigue failure of the insulated rail joints (IRJs)," *Engineering Failure Analysis,* vol. 40, pp. 58-74, 2014.

[6] R. Casciaro and G. Garcea, "An iterative method for shakedown analysis," *Computer Methods in Applied Mechanics and Engineering,* vol. 191, no. 49-50, pp. 5761-5792, 2002.

[7] G. Garcea, G. Armentano, S. Petrolo and R. Casciaro, "Finite element shakedown analysis of two-dimensional structures," *International Journal for Numerical Methods in Engineering,* vol. 63, no. 8, pp. 1174-1202, 28 6 2005.

[8] H. S. Yu, R. Salgado, S. W. Sloan and J. M. Kim, "Limit analysis versus limit equilibrium for slope stability," *Journal of Geotechnical and Geoenvironmental Engineering,* vol. 124, no. 1, pp. 1-11, 1998.

[9] A. R. S. Ponter and M. Engelhardt, "Shakedown limits for a general yield condition: Implementation and application for a Von Mises yield condition," *European Journal of Mechanics, A/Solids,* vol. 19, no. 3, pp. 423-445, 2000.

[10] G. Björkman and A. Klarbring, "Shakedown and residual stresses in frictional systems," *Contact Mechanics and Wear of Rail/Wheel Systems II: Proceedings of the 2nd International Symposium,* pp. 27-39, 1987.

[11] R. Seshadri and S. P. Mangalaramanan, "Lower bound limit loads using variational concepts: The mα-method," *International Journal of Pressure Vessels and Piping,* vol. 71, no. 2, pp. 93-106, 1997.

[12] A. Ponter, "An upper bound on the small displacements of elastic, perfectly plastic structures," *Journal of Applied Mechanics, Transactions ASME,* vol. 39, no. 4, pp. 959-963, 1972.

[13] A. R. S. Ponter and J. J. Williams, "Work bounds and associated deformation of cyclically loaded creeping structures," *Journal of Applied Mechanics, Transactions ASME,* vol. 40, no. 4, pp. 921-927, 1973.

[14] E.Melan, "Der Spannungenszustand eines Henky-Misesschen Kontinuums bei Veranderlicher Beelastung," *Sitzungsberichte der Accademic Wissenschaften,* pp. 147-173, 1938.

[15] F. Guarracino, G. Frunzio, V. Minutolo, L. G. Pan and L. Nunziante, "A theoretical approach and experimental results," in *AEPA 94*, Beijing, 1994.

[16] J. A. Koning, Shakedown of Elastic-Plastic Structures, Amsterdam, Oxford, New York, Tokyo: Elsevier, 1987.

[17] A. Ponter and J. Martin, "Some extremal properties and energy theorems for inelastic materials and their relationship to the deformation theory of plasticity," *Journal of the Mechanics and Physics of Solids,* vol. 20, no. 5, pp. 281-300, 1972.

[18] M.Capurso, "M. Capurso (1979) Some Upper Bound Principles to Plastic Strains in Dynamic Shakedown of Elastoplastic Structures, Journal of Structural Mechanics, 7:1, 1-20,," *Journal of Structural Mechanics,* pp. 1-20, 1979.

[19] G. Maier, "Complementary plastic work theorems in piecewise-linear elastoplasticity," *International Journal of Solids and Structures,* vol. 5, no. 3, pp. 261-270, 1969.

[20] V. Minutolo, E. Ruocco and M. Migliore, "On the influence of in-plane displacements on the stability of plate assemblies," *Journal of Strain Analysis for Engineering Design,* vol. 39, no. 2, pp. 213-223, 2004.

[21] E. Ruocco, V. Mallardo, V. Minutolo and D. Di Giacinto, "Analytical solution for buckling of Mindlin plates subjected to arbitrary boundary conditions," *Applied Mathematical Modelling,* vol. 50, pp. 497-508, 2017.

[22] J. Reyes and A. Chopra, Three-Dimensional Modal Pushover Analysis of Unsymmetric-Plan Buildings Subjected to Two Components of Ground Motion, vol. 24, 2013, pp. 203-217.